1521-0103/12/3403-629–637$25.00
THE JOURNAL OF PHARMACOLOGY AND EXPERIMENTAL THERAPEUTICS
Vol. 340, No. 3
188078/3749549
JPET 340:629–637, 2012

Prevention of Fibrosis Progression in CCl_4-Treated Rats: Role of the Hepatic Endocannabinoid and Apelin Systems

Vedrana Reichenbach, Josefa Ros, Guillermo Fernández-Varo, Gregori Casals, Pedro Melgar-Lesmes, Teresa Campos, Alexandros Makriyannis, Manuel Morales-Ruiz, and Wladimiro Jiménez

Service of Biochemistry and Molecular Genetics, Hospital Clínic, Barcelona, Spain (V.R., J.R., G.F.-V., G.C., P.M.-L., T.C., M.M.-R., W.J.); Institut d'Investigacions Biomèdiques August Pi i Sunyer, Barcelona, Spain (V.R., J.R., G.F.-V., P.M.-L., M.M.-R., W.J.); Centro de Investigación Biomédica en Red de Enfermedades Hepáticas y Digestivas, Barcelona, Spain (G.F.-V., M.M.-R., W.J.); Center for Drug Discovery, Northeastern University, Boston, Massachusetts (A.M.); and Department of Physiological Sciences I, University of Barcelona, Barcelona, Spain (W.J.)

Received September 15, 2011; accepted December 6, 2011

ABSTRACT

Endocannabinoids behave as antifibrogenic agents by interacting with cannabinoid CB2 receptors, whereas the apelin (AP) system acts as a proangiogenic and profibrogenic mediator in the liver. This study assessed the effect of long-term stimulation of CB2 receptors or AP receptor (APJ) blockade on fibrosis progression in rats under a non-discontinued fibrosis induction program. The study was performed in control and CCl_4-treated rats for 13 weeks. Fibrosis-induced rats received a CB2 receptor agonist (*R,S*)-3-(2-iodo-5-nitrobenzoyl)-1-(1-methyl-2-piperidinylmethyl)-1*H*-indole (AM1241) (1 mg/kg b.wt.), an APJ antagonist [Ala^{13}]-apelin-13 sequence: Gln-Arg-Pro-Arg-Leu-Ser-His-Lys-Gly-Pro-Met-Pro-Ala (F13A) (75 μg/kg b.wt.), or vehicle daily during the last 5 weeks of the CCl_4 inhalation program. Mean arterial pressure (MAP), portal pressure (PP), hepatic collagen content, angiogenesis, cell infiltrate, and mRNA expression of a panel of fibrosis-related genes were measured in all animals. Fibrosis-induced rats showed increased hepatic collagen content, reduced MAP, portal hypertension, and increased expression of the assessed messengers in comparison with control rats. However, fibrotic rats treated with either AM1241 or F13A had reduced hepatic collagen content, improved MAP and PP, ameliorated cell viability, and reduced angiogenesis and cell infiltrate compared with untreated fibrotic rats. These results were associated with attenuated induction of platelet-derived growth factor receptor β, α-smooth muscle actin, matrix metalloproteinases, and tissue inhibitors of matrix metalloproteinase. CB2 receptor stimulation or APJ blockade prevents fibrosis progression in CCl_4-treated rats. The mechanisms underlying these phenomena are coincident despite the marked dissimilarities between the CB2 and APJ signaling pathways, thus opening new avenues for preventing fibrosis progression in liver diseases.

Introduction

Inflammation and remodeling are orchestrated responses ultimately directed to promoting tissue repair after organ injury. However, maintenance of the injury results in the activation of a profibrogenic cascade of events in chronic liver disease that finally leads to cirrhosis. Cirrhosis is a major determinant of morbidity and mortality and predisposes to hepatic failure and primary liver cancer. Therefore, halting the progression of fibrosis to cirrhosis has largely been considered to be a foremost goal in patients with liver disease (Friedman, 2010). Inflammation is an early event in the history of the disease. It occurs before the onset of significant clinical manifestations and becomes chronic during the evolution of the illness, particularly in patients with viral infection (Marra, 1999). This dynamic inflammatory state has been associated with liver fibrogenesis and fibrosis in experimental cirrhosis (Muñoz-Luque et al., 2008). In addition,

This work was supported by the Dirección General de Investigación Científica y Técnica [Grants SAF09-08839, SAF07-63069] (to W.J. and M.M.-R., respectively); Agència de Gestió d'Ajuts Universitaris i de Recerca [Grant SGR 2009/1496]; Dirección General de Investigación Científica y Tecnológica [Grant BES-2004-5186] (to P.M.-L.); and Instituto de Salud Carlos III ["Contrato Post Formación Sanitaria Especializada" FIS CM07/00043] (to G.C.). Centro de Investigación Biomédica en Red-Enfermedades Hepáticas y Digestivas was founded by the Instituto de Salud Carlos III (Spain).

This work was previously presented in part at the following conferences: Reichenbach V, Ros J, Fernández-Varo G, Muñoz-Luque J, Morales-Ruiz M, Makriyannis A, and Jiménez W (2008) Chronic stimulation of cannabinoid CB2 receptor represses fibrosis progression in CCl_4-treated rats. *59th Annual Meeting of the American Association for the Study of Liver Diseases*; 2008 Oct 31–Nov 4; San Francisco, CA. American Association for the Study of Liver Diseases, Alexandria, VA. Reichenbach V, Ros J, Fernández-Varo G, Casals G, Melgar-Lesmes P, Pauta M, Morales-Ruiz M, and Jiménez W (2010) Activation of the hepatic apelin system is of major relevance in early stages of liver fibrosis. *International Liver Conference 2010*; 2010 Apr 14–18; Vienna, Austria. European Association for the Study of the Liver, Geneva, Switzerland.

Article, publication date, and citation information can be found at http://jpet.aspetjournals.org.

http://dx.doi.org/10.1124/jpet.111.188078.

many inflammatory mediators have direct angiogenic activities and, in turn, angiogenesis contributes to the perpetuation and the amplification of the inflammatory state by promoting the recruitment of inflammatory cells in the neovasculature (Morales-Ruiz and Jiménez, 2005; Tugues et al., 2007). Therefore, inflammation, fibrogenesis, and angiogenesis are three closely related phenomena in chronic liver disease.

Under this scenario, suitable targets for anti-fibroproliferative therapies should include molecules that are critical in fibrosis progression and also possess inflammatory and/or angiogenesis-related properties. In this regard, two recently characterized endogenous hepatic systems are attracting increasing attention, namely the hepatic endocannabinoid and apelin systems. Endocannabinoids are lipid-related molecules participating in a wide range of physiological functions including neuroprotection, pain and motor function, energy balance and food intake, cardiovascular homeostasis, immune and inflammatory responses, and cell proliferation (Pacher et al., 2006; Reichenbach et al., 2010; Tam et al., 2011). These effects are mediated by interaction with two different types of receptors, the CB1 and CB2 receptors. Of interest, the CB1 receptor in the liver has been shown to mediate profibrogenic effects (Teixeira-Clerc et al., 2006) and has also been implicated in the pathogenesis of alcoholic and nonalcoholic liver disease (Hézode et al., 2008; Jeong et al., 2008). On the other hand, CB2 receptor agonism shows opposite antifibrogenic and anti-inflammatory effects in hepatic and nonhepatic tissue (Muñoz-Luque et al., 2008; Akhmetshina et al., 2009) and protects against liver ischemia-reperfusion injury (Horváth et al., 2011). Previous studies by our laboratory have demonstrated that the proangiogenic peptide, apelin (AP), is up-regulated in HSCs of patients with cirrhosis (Melgar-Lesmes et al., 2010). Furthermore, this peptide behaves as a paracrine mediator of fibrogenesis-related gene induction in human HSCs (Melgar-Lesmes et al., 2010), and apelin receptor (APJ) blockade has shown to be effective in reducing hepatic fibrosis and angiogenesis in rats with cirrhosis (Principe et al., 2008). Recent studies have also suggested that the apelin system is involved in inflammation and in endothelial cell proliferation (Masri et al., 2004; Daviaud et al., 2006).

In the present investigation, we sought to examine new therapeutic strategies to prevent the progression of fibrosis in injured livers of rats chronically receiving increasing doses of CCl_4. We assessed the changes in messenger expression of a panel of genes involved in inflammation and/or tissue remodeling and the antifibrogenic, antiangiogenic, and anti-inflammatory effects induced by either long-term administration of a specific CB2 receptor agonist or a selective APJ receptor antagonist in rats with experimentally induced fibrosis.

Materials and Methods

Induction of Fibrosis in Rats. Studies were performed in 47 male adult Wistar rats (Charles River Laboratories, Saint Aubin les Elseuf, France). Rats with fibrosis ($n = 37$) and control rats ($n = 10$) were fed ad libitum with standard chow and water containing phenobarbital (0.3 g/l) as drinking fluid. Fibrosis was induced by CCl_4 inhalation as described previously (Clària and Jiménez, 1999). In brief, animals were exposed to a CCl_4 vapor atmosphere twice a week, starting at 0.5 min/exposure. The duration of the exposure was increased by 1 min after every three sessions until it reached 5 min, which was used until the end of the investigation. Rats with fibrosis were studied 13 weeks after the start of the fibrosis induction protocol. Control rats were studied after a similar period of phenobarbital administration. The study was performed according to the criteria of the investigation and ethics committees of the Hospital Clínic Universitari.

Selective Activation of CB2 Receptors in Fibrotic Rats. The hemodynamic and gene expression effects of CB2 receptor activation were assessed in 20 rats with fibrosis. Ten animals were randomly assigned to a daily subcutaneous injection of a specific CB2 agonist, (*R,S*)-3-(2-iodo-5-nitrobenzoyl)-1-(1-methyl-2-piperidinylmethyl)-1*H*-indole (AM1241) at a dose of 1 mg/kg per day b.wt.) (Malan et al., 2001). In parallel, 10 rats received a solution of ethanol-Cremophor ELP-saline (1:1:18) as vehicle. AM1241 or vehicle was administered from the 9th to the 13th week after the start of the fibrosis induction protocol.

APJ Blockade in Fibrotic Rats. The hemodynamic and gene expression effects of APJ blockade were assessed in 17 rats with fibrosis. Seven animals were randomly assigned to a daily subcutaneous injection of an APJ antagonist, [Ala^{13}]-apelin-13 sequence: Gln-Arg-Pro-Arg-Leu-Ser-His-Lys-Gly-Pro-Met-Pro-Ala (F13A) at a dose of 75 μg/kg per day b.wt. (Phoenix Pharmaceuticals, Belmont, CA), and 10 rats received 1 ml/kg per day of saline solution as vehicle. F13A or vehicle was administered from the 9th to the 13th week after the start of the fibrosis induction protocol.

Hemodynamic Studies. Rats with fibrosis and control rats were anesthetized with Inactin (50 mg/kg b.wt.; Sigma-Aldrich Chemie GmbH, Taufkirchen, Germany) and prepared with a polyvinyl-50 catheter in the left femoral artery. The animals were prepared for measurements of hemodynamic parameters as described previously (Ros et al., 2005). Hemodynamic parameters were allowed to equilibrate for 30 min, and values of mean arterial pressure (MAP), portal pressure (PP), and heart rate were recorded. Splanchnic perfusion pressure (SPP) was defined as MAP − PP. At the end of the study, the animals were exsanguinated and a blood sample (6–9 ml) was taken to measure standard parameters of hepatic and renal function.

Quantification of Fibrosis and Apoptosis in Hepatic Tissue. Liver sections (4 μm) were stained in 0.1% Sirius red F3B (Sigma-Aldrich Chemie GmbH) in saturated picric acid (Sigma-Aldrich Chemie GmbH). Relative fibrosis area (expressed as a percentage of total liver area) was assessed by analyzing 32 fields of Sirius red-stained liver sections per animal. Each field was acquired at 10× magnification (Eclipse E600; Nikon, Kawasaki, Kanagawa, Japan) and then analyzed using the morphometry software ImageJ (version 1.37). To evaluate the relative fibrosis area, the collagen area measured was divided by the net field area and then multiplied by 100. Subtraction of vascular luminal area from the total field area yielded the final

ABBREVIATIONS: AP, apelin; HSC, hepatic stellate cell; APJ, apelin receptor; AM1241, (*R,S*)-3-(2-iodo-5-nitrobenzoyl)-1-(1-methyl-2-piperidinylmethyl)-1*H*-indole; F13A, [Ala^{13}]-apelin-13 sequence: Gln-Arg-Pro-Arg-Leu-Ser-His-Lys-Gly-Pro-Met-Pro-Ala; MAP, mean arterial pressure; PP, portal pressure; SPP, splanchnic perfusion pressure; TUNEL, terminal deoxynucleotidyl transferase dUTP nick-end labeling; PDGFRβ, platelet-derived growth factor receptor β; TGFβR1, transforming growth factor β receptor 1; Col1α2, collagen-Iα2; α-SMA, α-smooth muscle actin; TIMP, tissue inhibitor of matrix metalloproteinase; MMP, matrix metalloproteinase; HPRT, hypoxanthine guanine phosphoribosyltransferase; vWF, von Willebrand factor; AST, aspartate aminotransferase; ALT, alanine aminotransferase; ANOVA, analysis of variance; ECM, extracellular matrix; PDGF, platelet-derived growth factor; Col1, collagen type 1; C_T, comparative threshold cycle.

calculation of the net fibrosis area. The amount of fibrosis measured in each animal was analyzed, and the average value is presented as a percentage.

To determine the degree of hepatic apoptosis, we used the terminal deoxynucleotidyl transferase dUTP nick-end labeling (TUNEL) assay to detect cell death using a fluorescein-FragEL DNA Fragmentation Detection Kit (Calbiochem, San Diego, CA) according to the manufacturer's protocol. To quantify and compare the rates of cell death between groups, a semiquantitative scoring method was used. For each sample, the number of TUNEL-positive cells was counted per 200× high-power field. At least eight representative fields were evaluated for each experimental group, from which an average value was calculated.

Hepatic Messenger Expression of a Panel of Profibrogenic Genes in Fibrotic Rats. Liver specimens were obtained from each animal, washed in 0.1% diethyl pyrocarbonate-treated phosphate-buffered saline salt solution (140 mM NaCl, 8.5 mM Na_2HPO_4, and 1.84 mM $Na_2HPO_4 \cdot H_2O$, pH 7.4), immediately frozen in dry ice, and stored in liquid nitrogen. Liver samples from treated and untreated animals were also fixed in 10% buffered formalin for further hematoxylin and eosin and immunostaining analysis. Total RNA was extracted from the middle liver lobe of control and fibrotic rats using a commercially available kit (RNAeasy; QIAGEN, Hilden, Germany). The RNA concentration was determined by spectrophotometric analysis (ND-100 spectrophotometer; Thermo Fisher Scientific, Waltham, MA). One microgram of total RNA was reverse-transcribed using a cDNA synthesis kit (High-Capacity cDNA Reverse Transcription Kit; Applied Biosystems, Foster City, CA). Specific primers and probes used for the different genes studied were designed to include intron spanning using the Universal ProbeLibrary Assay Design Center through ProbeFinder version 2.45 software (Roche Diagnostics, Indianapolis, IN; https://www.roche-applied-science.com/sis/rtpcr/upl/index.jsp). A panel of selected profibrogenic genes was analyzed. The panel included the following: platelet-derived growth factor receptor β (PDGFRβ) (probe 69; left 5′-GCGGAAGCGCATCTATATCT-3′ and right 5′-GCGGAAGCGCATCTATATCT-3′), transforming growth factor β receptor 1 (TGFβR1) (probe 53; left 5′-AAGGCCAAATATTCCCAACA-3′ and right 5′-ATTTTGGCCATCACTCTCAAG-3′), collagen-Iα2 (Col1α2) (probe 95; left 5′-AGACCTGGCGAGAGAGGAGT-3′ and right 5′-ATCCAGACCGTTGTGTCCTC-3′), α-smooth muscle actin (α-SMA) (probe 78; left 5′-CATCAGGAACCTCGAGAAGC-3′ and right 5′-AGCCATTGTCACACACCAGA-3′), tissue inhibitor of matrix metalloproteinases type 1 (TIMP1) (probe 95; left 5′-CATGGAGAGCCTCTGTGGAT-3′ and right 5′-TGTGCAAATTTCCGTTCCTT-3′), TIMP2 (probe 73; left 5′-GACAAGGACATCGAATTTATCTACAC-3′ and right 5′-CCATCTCCTTCCGCCTTC-3′), matrix metalloproteinase 2 (MMP2) (probe 60; left 5′-CTCCACTACGCTTTTCTCGAAT-3′ and right 5′-TGGGTATCCATCTCCATGCT-3′), and MMP9 (probe 53; left 5′-CCTGAAAACCTCCAACCTCA-3′ and right: 5′-GAGTGTAACCATAGCGGTACAGG-3′). Hypoxanthine-guanine phosphoribosyltransferase (HPRT) (probe 95: left 5′-GACCGGTTCTGTCATGTCG-3′ and right 5′-ACCTGGTTCATCATCACTAATCAC-3′) was used as the reference gene. Primers were designed according to rat sequences (GenBank codes NM_031525.1, NM_012775.2, NM_053356.1, NM_031004.2, NM_053819.1, NM_021989.2, NM_031054.2, NM_031055.1, and NM_012583.2, respectively). Real-time quantitative polymerase chain reaction was analyzed in duplicate and performed with the LightCycler 480 (Roche Diagnostics). A 10-μl total volume reaction of diluted 1:8 cDNA, 200 nM primer dilution, 100 nM prevalidated 9-mer probe (Universal ProbeLibrary) and FastStart TaqMan Probe Master (Roche Diagnostics) were used in each polymerase chain reaction reaction. A fluorescence signal was captured during each of the 45 cycles (denaturizing for 10 s at 95°C, annealing for 20 s at 60°C, and extension for 1 s at 72°C). HPRT was used as a reference gene for normalization, and water was used as a negative control. Relative quantification was calculated using the comparative threshold cycle (C_T), which is inversely related to the abundance of mRNA transcripts in the initial sample. The mean C_T of duplicate measurements was used to calculate ΔC_T as the difference in C_T for target and reference. The relative quantity of product was expressed as fold induction of the target gene compared with the reference gene according to the formula $2^{-\Delta\Delta C_T}$, where $\Delta\Delta C_T$ represents ΔC_T values normalized with the mean ΔC_T of control samples.

Western Blot Analysis of Activated Caspase-3, PDGFRβ, and TIMP1. Hepatic tissue from treated and nontreated rats was individually homogenized as described previously (Muñoz-Luque et al., 2008). To detect PDGFRβ, TIMP1, and activated caspase-3, 80 μg of total denatured proteins were loaded on a 7% (PDGFRβ) and 12% (TIMP1 and caspase-3) SDS-polyacrylamide gel (Mini-PROTEAN III; Bio-Rad Laboratories, Hercules, CA). Gels were transferred for 2 h to nitrocellulose membranes of 0.45 μm for PDGFRβ and to 0.2 μm for TIMP1 and caspase-3 and blocked with 5% nonfat milk for PDGFRβ and 1% bovine serum albumin for TIMP1 and caspase-3 in TTBS buffer at room temperature for 2 h. All membranes were stained with Ponceau S Red as a control for protein loading and were then incubated overnight at 4°C with rabbit polyclonal anti-PDGFRβ (1:1000; Cell Signaling Technology, Danvers, MA), anti-TIMP1 (1:1000; Abcam, Cambridge, UK), and anti-activated caspase-3 (1:300 dilution; Abcam) for 24, 24, or 48 h, respectively. The bands were visualized by chemiluminescence (Lumi-Light Western blotting substrate; Roche Diagnostics).

Immunodetection of CD68 and von Willebrand Factor. Liver sections from cirrhotic rats underwent microwave antigen retrieval to unmask antigens hidden by cross-linkage occurring during tissue fixation. Endogenous peroxidase activity was blocked by hydrogen peroxide pretreatment for 10 min and with 5% goat serum for 45 min. The sections were then stained with mouse anti-CD68 (1:150; AbD Serotec, Oxford, UK) or with rabbit anti-vWF (1:500; Dako Denmark A/S, Glostrup, Denmark) and incubated for 1 h at room temperature or overnight at 4°C, respectively. The LSAB 2 System-HRP (Dako Denmark A/S) was used for antigen detection, and antigen visualization was achieved with streptavidin peroxidase and counterstained with hematoxylin.

Measurements and Statistical Analysis. Serum osmolality was determined from osmometric depression of the freezing point (Osmometer 3300; Advanced Instruments, Needham Heights, MA) and Na^+ and K^+ concentrations by flame photometry (IL 943; Instrumentation Laboratory, Lexington, MA). Serum albumin, aspartate aminotransferase (AST), alanine transaminase (ALT), and lactate dehydrogenase were measured with the ADVIA 2400 Instrument (Siemens Healthcare Diagnostics, Tarrytown, NY). Quantitative data were analyzed using GraphPad Prism 5 (GraphPad Software, Inc., San Diego, CA), and statistical analysis of the results was performed by one-way analysis of variance (ANOVA) with the Newman-Keuls post hoc test and the Kruskal-Wallis test with the Dunn post hoc test when appropriate. Data are expressed as means ± S.E.M. and were considered significant at $p < 0.05$.

Results

Liver Function Tests, Mean Arterial Pressure, and Portal Pressure in Treated and Nontreated Fibrotic Rats. Table 1 shows the biochemical tests of liver function, serum electrolytes, and systemic hemodynamics in fibrotic rats. As anticipated, in both experimental groups, fibrotic animals receiving vehicle showed the characteristic alterations of liver function tests, arterial hypotension, and significant portal hypertension. Chronic administration of the CB2 receptor agonist resulted in an approximately 50% reduction of ALT and AST levels in serum. No any other significant effects were observed in the biochemical parameters measured between vehicle-treated rats and rats receiving either the CB2 receptor agonist or the APJ antagonist. Of note,

TABLE 1

Body weight, standard liver function, serum electrolytes, and systemic hemodynamics in fibrotic rats receiving vehicle or treated with the CB2 agonist AM1241 or the APJ antagonist F13A

Results are given as means ± S.E.

Parameter	Control (n = 10)	CCl_4-Treated Rats			
		CB2 Stimulation		APJ Blockade	
		Vehicle (n = 10)	AM1241 (n = 10)	Vehicle (n = 10)	F13A (n = 7)
Body weight, g	399 ± 8	415 ± 7	403 ± 12	379 ± 10	380 ± 7
AST, U/l	117 ± 23	582 ± 58†††	295 ± 46***	373 ± 72††	431 ± 113
ALT, U/l	12.8 ± 1	326 ± 29†††	199 ± 60*	276 ± 89††	282 ± 46
Lactate dehydrogenase, U/l	1093 ± 106	1127 ± 94	1176 ± 344	1016 ± 178	1851 ± 619
Albumin, g/l	36.1 ± 0.5	29.3 ± 1.5†††	30.5 ± 0.7	29.2 ± 0.96†††	30.1 ± 0.8
Serum Na^+, mEq/l	142 ± 1.6	141 ± 1	142 ± 1	142 ± 1	143 ± 1
Serum K^+, mEq/l	5.1 ± 0.2	4.9 ± 0.2	4.9 ± 0.1	4.7 ± 0.2	5.0 ± 0.2
Serum osmolality, mOsmol/kg	292 ± 6	296 ± 1	296 ± 2	303 ± 3	302 ± 3
MAP, mm Hg	121 ± 1	111 ± 3††	126 ± 2**	110 ± 3††	124 ± 2**
PP, mm Hg	5.6 ± 0.2	10.2 ± 0.4†††	7.6 ± 0.8**	11.3 ± 0.6†††	7.5 ± 0.6***
SPP, mm Hg	117 ± 2	99 ± 3†††	117 ± 4***	100 ± 4†††	116 ± 2*
Heart rate, beats/min	395 ± 15	399 ± 13	424 ± 8	410 ± 12	421 ± 8

* $p < 0.05$, compared with vehicle-treated rats (one-way ANOVA with the Newman-Keuls post hoc test and the Kruskal-Wallis test with the Dunn post hoc test when appropriate).
** $p < 0.01$.
*** $p < 0.001$.
† $p < 0.001$, compared with control rats.
†† $p < 0.01$.
††† $P < 0.001$.

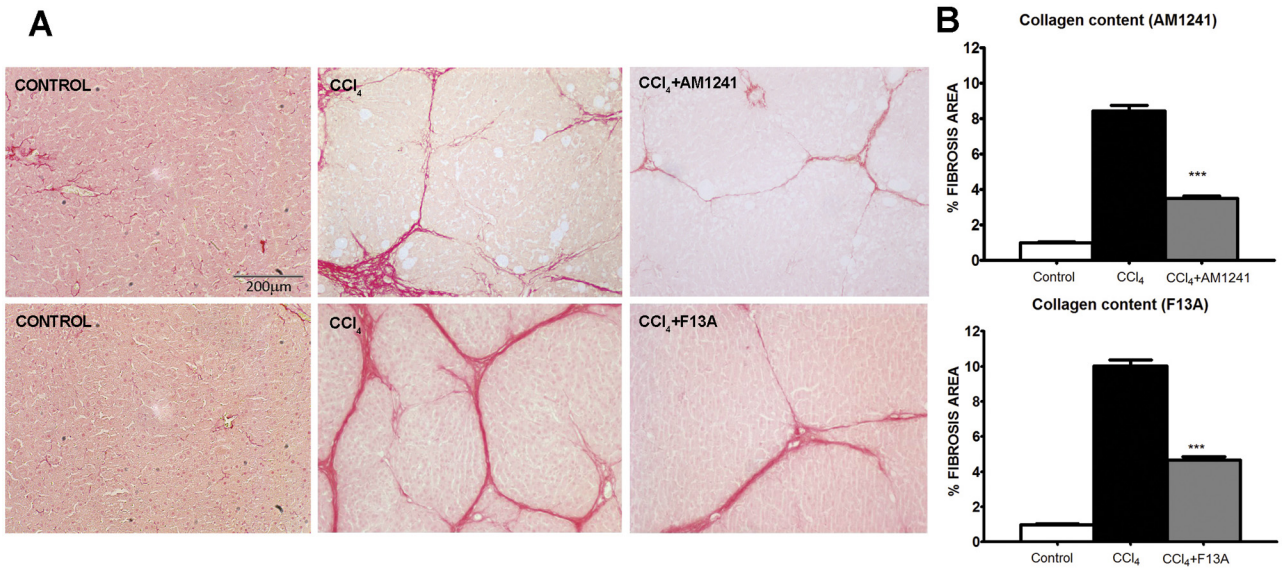

Fig. 1. A, effect of CB2 receptor activation (AM1241) and APJ blockade (F13A) on liver fibrosis. Sirius red staining of representative liver sections obtained from control rats, rats treated with vehicle, and rats receiving AM1241 (1 mg/kg per day b.wt.) or F13A (75 µg/kg per day b.wt.). Original magnification, 100×. Quantification of relative fibrosis area was assessed in 32 fields/animal. B, bars on the right show the quantitative measurement of relative fibrosis in all the animals. Results are given as means ± S.E. ***, $p < 0.001$.

however, long-term administration of AM1241 and F13A was associated with a significant amelioration in hemodynamic function as reflected by higher MAP and SPP and lower PP in fibrotic treated rats than in fibrotic rats receiving vehicle.

Effect of CB2 Receptor Activation and APJ Blockade on Liver Fibrosis in Fibrotic Rats. Sirius red, a dye that selectively binds collagen proteins, was used to stain the collagen fibrils in the liver of CCl_4-treated rats (Jiménez et al., 1985). As shown in Fig. 1, both groups of rats had remarkable fibrosis showing initial stages of the characteristic pattern of perivenular and periportal deposition of connecting tissue with development of thin portal-to-portal septa and slight evidence of architectural distortion resulting in micronodular fibrosis. However, biopsy samples obtained from fibrotic rats receiving AM1241 and from fibrotic rats receiving F13A displayed thinner septa and more preserved hepatic parenchyma than those from nontreated fibrotic animals. This result was confirmed by the morphometric analysis of all Sirius red-stained sections in which both hepatic samples of rats collected after CB2 receptor stimulation and liver biopsy samples obtained after APJ blockade showed a significant reduction in the percentage of fibrosis area compared with that in sections of the corresponding vehicle-treated fibrotic rats (Fig. 1).

Effects of CB2 Receptor Activation and APJ Blockade on Infiltrating Cells, Vessel Density, Apoptosis, and Activated Caspase-3 Expression. To assess the density of infiltrating macrophages/monocytes in the liver tissue of both vehicle and treated rats, CD68-positive cells were quantified in the parenchymal area and the periportal area. The amount of in-

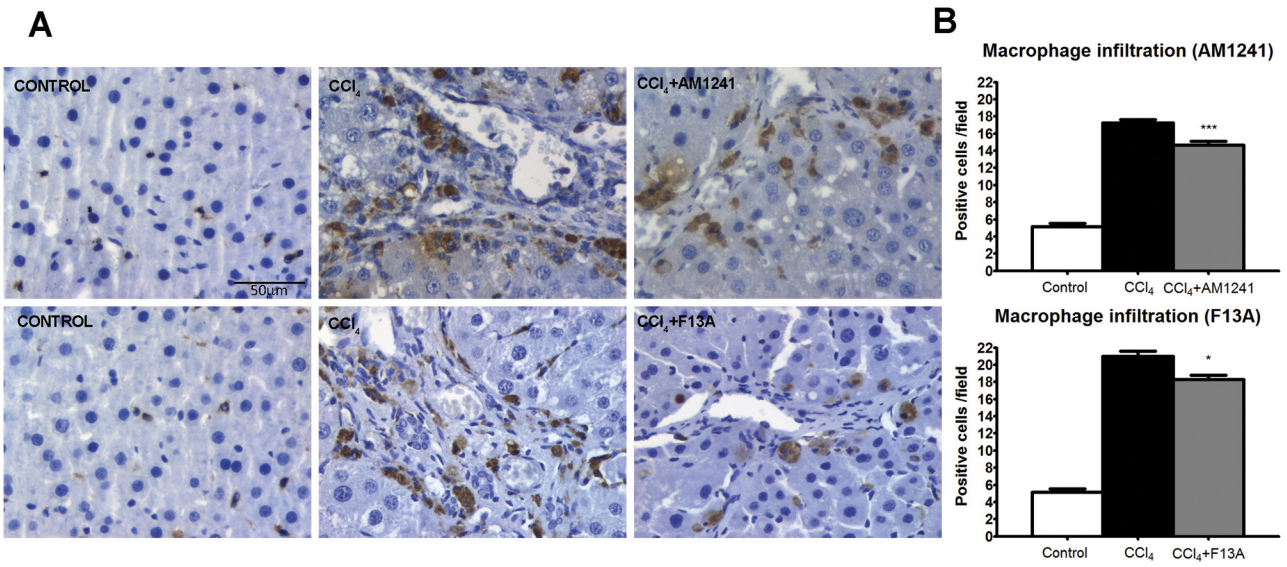

Fig. 2. A, effect of CB2 receptor activation (AM1241) and APJ blockade (F13A) on infiltrating cells. CD68 staining of representative liver sections obtained from control rats, rats treated with vehicle, and rats receiving AM1241 (1 mg/kg per day b.wt.) or F13A (75 μg/kg per day b.wt.). Positive cells were determined by counting the number of CD68-positive stained cells in 20 independent fields/animal. Original magnification, 400×. B, bars on the right show the quantitative measurement of infiltrating cells in all the animals. Results are given as means ± S.E. *, $p < 0.05$; ***, $p < 0.001$.

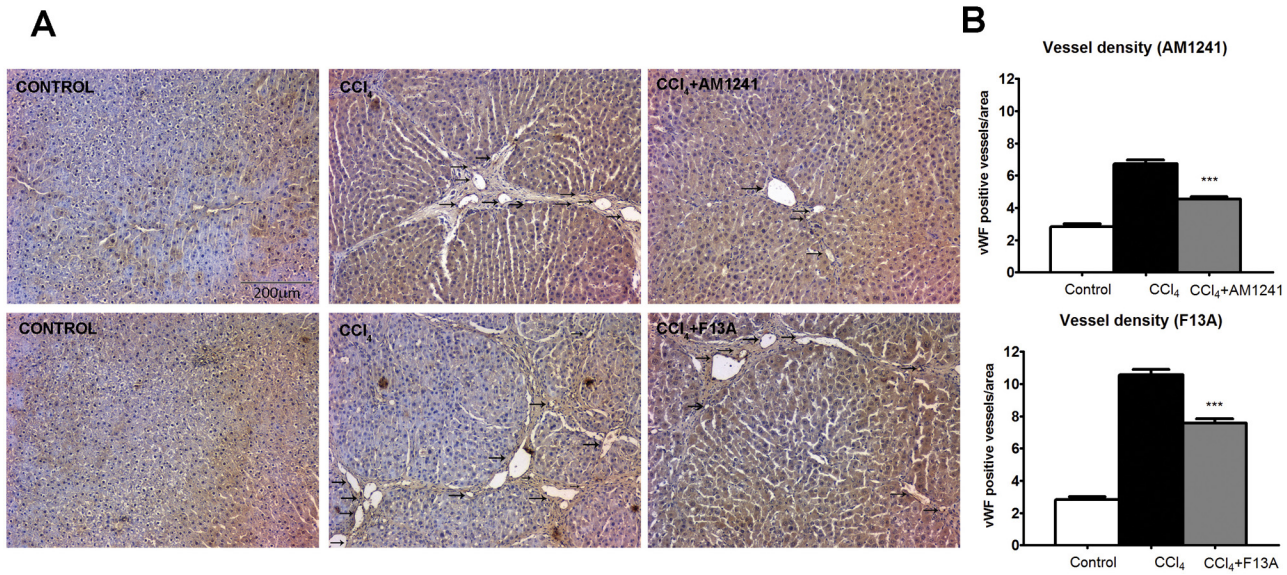

Fig. 3. A, effect of CB2 receptor activation (AM1241) and APJ blockade (F13A) on vessel density. Immunolocalization of vWF was used to quantify vessel density in liver sections obtained from control rats, rats receiving vehicle, or rats treated with either AM1241 (1 mg/kg per day b.wt.) or F13A (75 μg/kg per day b.wt.). Positive staining was determined counting vWF-positive stained vessels in 20 independent fields/animal. Original magnification, 100×. B, bars on the right show the quantitative measurement of vessel density in all animals. Results are given as means ± S.E. ***, $p < 0.001$.

filtrated cells was significantly higher in CCl_4-treated rats compared with that in controls. Chronic treatment with the CB2 receptor agonist or the APJ antagonist significantly decreased the number of CD68-positive cells in the liver of fibrotic rats (Fig. 2). Next, to evaluate whether AM1241 or F13A treatment may exert an antiangiogenic effect, anti-vWF antibody was used to quantify the number of vessels. There was a significant decrease in the amount of blood vessels in both AM1241- and F13A-treated animals compared with that for vehicle (Fig. 3). To explore whether antifibrogenic treatments may modify apoptosis, we performed in situ detection of nuclear DNA fragmentation by the TUNEL assay in liver sections of treated and nontreated fibrotic rats. As a positive control of the TUNEL assay, apoptosis was induced by incubation of liver sections with DNase I. No staining was observed in the negative control in which the terminal deoxynucleotidyl transferase enzyme was omitted (data not shown). Liver sections from fibrotic rats showed positive TUNEL staining cells with immunoreactivity localized to the margin of the fibrous septa and parenchyma (Fig. 4). However, the number of positive cells for TUNEL staining significantly decreased in hepatic sections of animals treated with AM1241 and F13A compared with the vehicle group (6 ± 1 versus 3 ± 0 positive cells/field, $p < 0.001$ and 5 ± 0 versus 3 ± 1 positive cells/field, $p < 0.001$, respectively). Finally, we measured the amount of active caspase-3 in livers of control, vehicle-treated, AM1241-treated, or F13A-treated animals. As shown in Fig. 4, the amount of activated caspase-3 was significantly higher in fibrotic rats than in controls. Of interest,

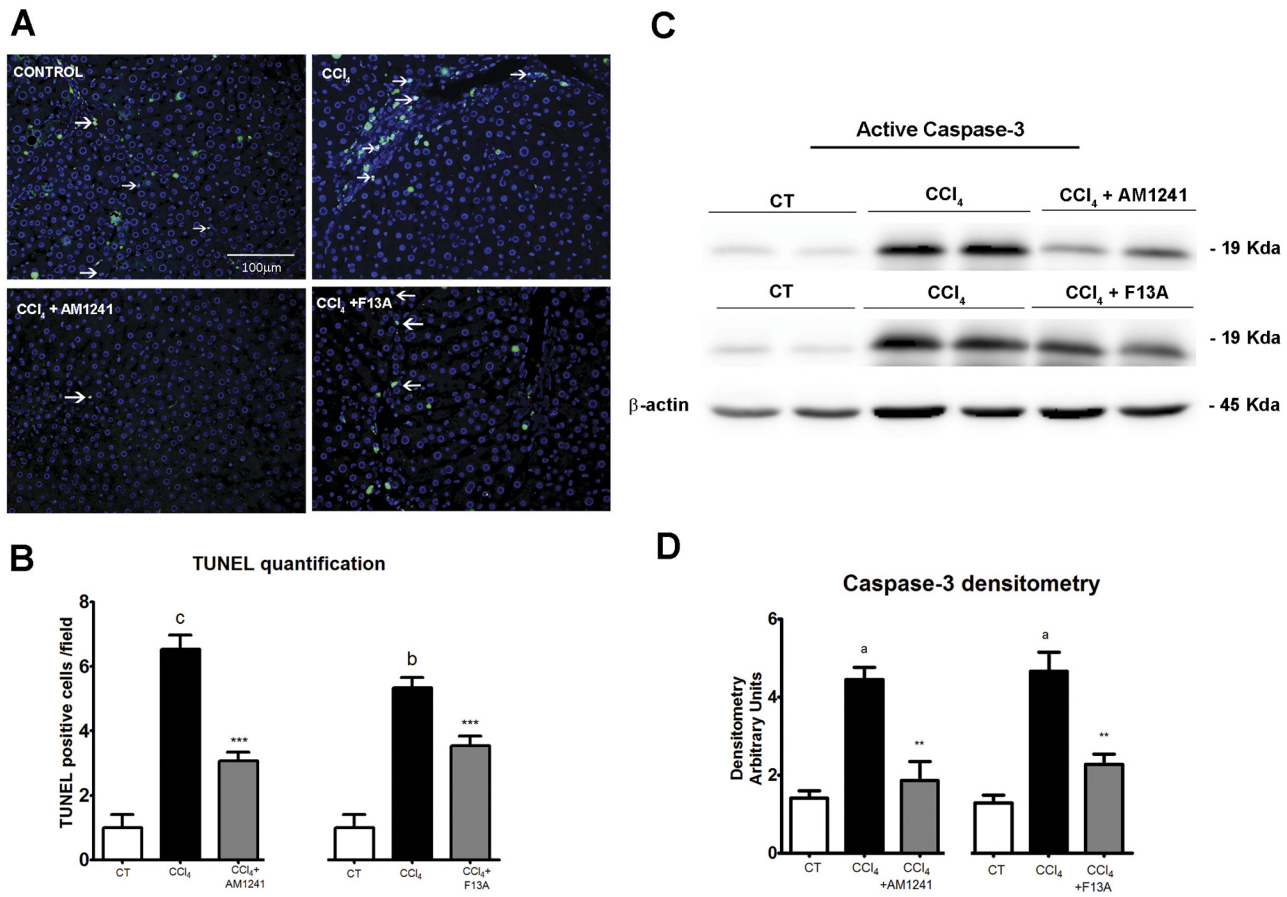

Fig. 4. Effect of CB2 receptor activation and APJ blockade on apoptosis. A, representative TUNEL assay in hepatic tissue of control rats and fibrotic rats receiving vehicle (CCl_4) or treated with the CB2 receptor agonist (CCl_4 + AM1241) or the APJ antagonist (CCl_4 + F13A). The number of positive cells was determined by counting the number of positively stained cells in eight independent fields per animal (original magnification, 200×). B, bars at the bottom show the quantitative measurement of TUNEL-positive cells in all animals. C, Western blot for activated caspase-3 on liver tissue of control rats (CT), fibrotic rats receiving vehicle (CCl_4), and fibrotic rats treated with either AM1241 (CCl_4 + AM1241, 1 mg/kg per day b.wt.) or F13A (CCl_4 + F13A, 75 μg/kg per day b.wt.) for 5 weeks. Eighty micrograms of protein was loaded per lane. D, bars at the bottom show the densitometric analysis of all the samples normalized to β-actin. Results are given as means ± S.E. a, $p < 0.05$; b, $p < 0.01$; c, $p < 0.001$ versus control; **, $p < 0.01$; ***, $p < 0.001$ versus CCl_4.

both CB2 receptor stimulation and APJ blockade significantly reduced activated caspase-3 expression in the hepatic tissue of fibrotic rats. These findings indicate that chronic in vivo CB2 stimulation or APJ blockade prevents proangiogenic and apoptotic phenomena in the liver of CCl_4-induced fibrotic rats.

TABLE 2

Gene expression of PDGFRβ, TGFβR1, Col1α2, α-SMA, MMP2, MMP9, TIMP1, and TIMP2, measured in the hepatic tissue of reference control rats and in fibrotic rats receiving vehicle or treated with the CB2 agonist AM1241 or the APJ antagonist F13A

Results are given as means ± S.E.

Genes (*fold change*)	Control (n = 10)	CCl_4-Treated Rats			
		CB2 Stimulation		APJ Blockade	
		Vehicle (n = 10)	AM1241 (n = 10)	Vehicle (n = 10)	F13A (n = 7)
PDGFRβ	1.02 ± 0.11	3.74 ± 0.81†	1.22 ± 0.27**	4.87 ± 0.92†††	2.36 ± 0.37*
TGFβR1	1.08 ± 0.21	1.46 ± 0.40	0.64 ± 0.06	2.05 ± 0.15*,†	1.81 ± 0.35
Col1α2	1.04 ± 0.12	9.40 ± 1.31††	7.42 ± 1.61	9.80 ± 1.95†††	6.23 ± 1.39
α-SMA	1.10 ± 0.02	9.19 ± 1.70††	3.57 ± 0.89**	6.39 ± 0.48†	2.27 ± 1.30*
MMP2	0.97 ± 0.08	8.13 ± 1.39††	4.35 ± 0.82*	9.49 ± 1.23††	5.56 ± 0.73*
MMP9	1.04 ± 0.07	20.05 ± 4.12††	23.5 ± 5.42	14.46 ± 3.88††	14.32 ± 1.18
TIMP1	1.05 ± 0.18	12.42 ± 1.90††	6.28 ± 1.10**	8.97 ± 1.39†††	3.43 ± 0.56**
TIMP2	1.02 ± 0.08	3.11 ± 0.35†††	1.89 ± 0.15**	3.56 ± 0.53††	2.42 ± 0.36

* $p < 0.05$, compared with vehicle-treated rats (one-way ANOVA with the Newman-Keuls post hoc test and the Kruskal-Wallis test with the Dunn post hoc test when appropriate).
** $p < 0.01$.
*** $p < 0.001$.
† $p < 0.05$, compared with control rats.
†† $p < 0.01$.
††† $p < 0.05$.

Effect of CB2 Receptor Activation and APJ Blockade on mRNA of Hepatic Profibrogenic Genes and Protein Expression of PDGFRβ and TIMP1. For further insight into the effect of AM1241 and F13A in fibrotic rats, we measured hepatic mRNA expression of a panel of selected genes involved in cytokine signaling (TGFβR1 and PDGFRβ), collagen synthesis (Col1α2), stellate cell activation (α-SMA), and extracellular matrix (ECM) turnover (MMP2, MMP9, TIMP1, and TIMP2) (Table 2). After 13 weeks of CCl_4 treatment, all the genes analyzed were up-regulated in fibrotic rats compared with control animals. TGFβR1 was the least, albeit significantly, activated transcript (approximately a 2-fold increase), whereas the most intensely up-regulated messengers were those related to ECM turnover, such as MMP9 and TIMP1. The antifibrogenic properties displayed by AM1241 and F13A were paralleled by a decrease in mRNA expression in these genes. In fact, both the CB2 agonist and the APJ antagonist inhibited PDGFRβ expression and significantly reduced the degree of activation of HSCs as shown by the decrease in the mRNA expression of α-SMA. However, the most interesting finding was that both treatments significantly altered the expression balance of the transcripts involved in ECM turnover, thus favoring ECM degradation. In fact, although neither AM1241 nor F13A treatment modified MMP9 expression, both compounds induced a significant reduction in TIMP abundance, which, in turn, resulted in a marked increase in the MMP/TIMP gene expression ratio (Table 3).

Because inhibition of mRNA expression of PDGFRβ and TIMP1 appeared to be major contributory factors to the antifibrotic properties of both AM1241 and F13A treatments, we next assessed whether CB2 receptor stimulation or APJ blockade was also associated with lower hepatic abundance of PDGFRβ and TIMP1 proteins. As shown in Fig. 5, PDGFRβ and TIMP1 expression were significantly reduced in fibrotic rats treated with AM1241 or F13A compared with fibrotic animals treated with vehicle.

TABLE 3

MMP/TIMP ratios calculated from the mRNA expression of MMP2, MMP9, TIMP1, and TIMP2 in liver tissue of fibrotic rats receiving vehicle or treated with the CB2 agonist AM1241 or the APJ antagonist F13A

Results are given as means ± S.E.

Gene Ratio	CCl_4-Treated Rats			
	CB2 Stimulation		APJ Blockade	
	Vehicle	AM1241	Vehicle	F13A
MMP2/TIMP1	0.91 ± 0.24	0.88 ± 0.21	1.43 ± 0.27	1.56 ± 0.12
MMP2/TIMP2	2.66 ± 0.48	2.18 ± 0.27	2.80 ± 0.26	2.09 ± 0.13
MMP9/TIMP1	1.79 ± 0.40	4.56 ± 0.96*	2.13 ± 0.54	4.91 ± 1.0*
MMP9/TIMP2	6.75 ± 1.36	15.7 ± 3.47*	4.39 ± 1.04	9.14 ± 3.35

* $p < 0.05$; unpaired Student's t test.

Discussion

The results of this investigation indicate that chronic administration of either AM1241 or F13A reduces hepatic collagen deposition in rats under a non-discontinued fibrosis induction program. These findings indicate that long-term CB2 receptor stimulation or signaling disruption of the hepatic apelin system prevents fibrosis progression in CCl_4-

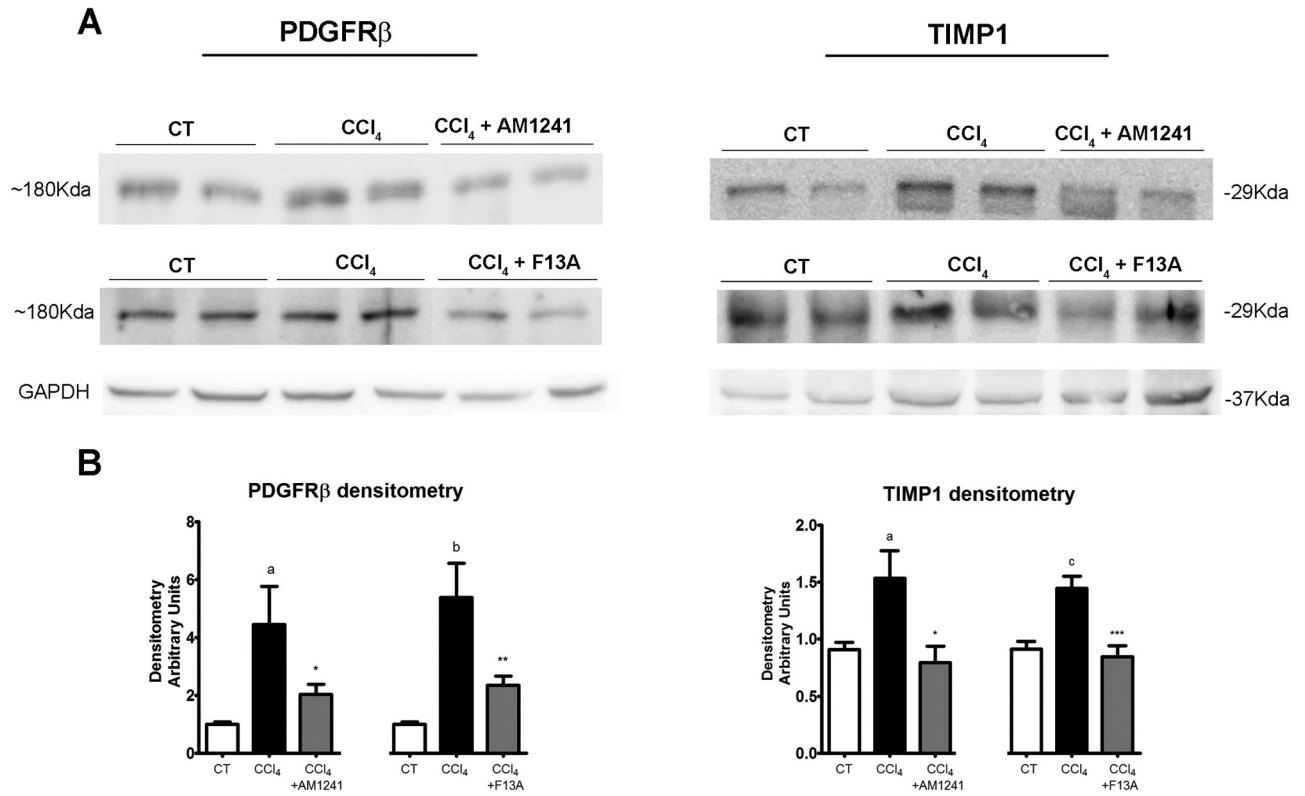

Fig. 5. A, effect of CB2 receptor activation and APJ blockade on protein expression of PDGFRβ and TIMP1. Representative Western blot for PDGFRβ and TIMP1 in liver tissue of control rats (CT), fibrotic rats receiving vehicle (CCl_4), and fibrotic rats treated with either AM1241 (CCl_4 + AM1241, 1 mg/kg per day b.wt.) or F13A (CCl_4 + F13A, 75 μg/kg per day b.wt.) for 5 weeks. Eighty micrograms of protein was loaded per lane. B, bars at the bottom show the densitometric analysis of all the samples normalized to GAPDH. Results are given as means ± S.E. a, $p < 0.05$; b, $p < 0.01$; c, $p < 0.001$ versus control; *, $p < 0.05$; **, $p < 0.01$; ***, $p < 0.001$ versus CCl_4.

treated rats. Our results also indicate that the molecular mechanisms ultimately underlying these phenomena are coincident despite the marked dissimilarities between the CB2 and APJ signaling pathways, thus opening new avenues for preventing fibrosis progression in liver diseases.

In fact, the chronic administration of either AM1241 or F13A to rats under a CCl_4-induced fibrosis/cirrhosis protocol resulted in significantly decreased hepatic collagen deposition, which was associated with a significant amelioration in systemic and portal hemodynamics, reduced angiogenesis, inflammatory infiltrate, and apoptosis compared with that in rats under the same fibrosis induction protocol but treated with vehicle. Moreover, animals receiving the CB2 agonist also showed signs of attenuated liver inflammation as indicated by decreased serum AST and ALT enzymes. All these changes were framed by reduced expression of messengers related to PDGF signaling, HSC activation, and ECM turnover.

Our group and others have previously described the antifibrogenic properties of CB2 receptor stimulation in experimental models of advanced liver disease (Julien et al., 2005; Liu et al., 2008; Muñoz-Luque et al., 2008). Whereas the experimental design of these studies focused on fibrosis regression, here we assessed whether CB2 agonism is able to prevent fibrosis progression even under conditions of maintaining the hepatic injury. We administered the CB2 receptor agonist AM1241 to rats under a fibrosis induction protocol. AM1241 is among the most selective receptor agonists currently available. For CB2 and CB1 receptors, the binding affinity (K_i) is 3.4 and 239.4 nM, respectively, and previous experiments have provided pharmacological and biochemical evidence that AM1241 selectively activates the CB2 receptor in vivo in mice, rats, and human cell lines (Malan et al., 2001; Ibrahim et al., 2003; Yao et al., 2006). The absence of central effects induced by CB2 agonism has been the major rationale to propose this mechanism as an antifibrogenic therapy. However, previous studies showed that pharmacological activation of the CB2 receptor signaling pathway may also induce inflammation in adipose tissue but not in the liver (Deveaux et al., 2009). In agreement with these findings, treatment with the CB2 agonist, in addition to stopping fibrosis progression and angiogenesis, was also associated with decreased serum levels of AST and ALT and reduced inflammatory infiltrate. An interesting finding of this study was that in contrast to what we had previously found in cirrhotic rats (Muñoz-Luque et al., 2008), administration of AM1241 inhibited apoptosis in fibrotic animals. Although we do not have any experimental data to explain this phenomenon, we believe that it is probably related to the different degrees of active fibrogenesis between the two groups of CCl_4-treated animals. In fact, in the former study, the rats had fully established cirrhosis and the active fibrogenesis was much lower than that in the animals of the current investigation that were within the initial phases of fibrosis development (Gressner et al., 2007; Iredale, 2007). There are a number of potential mechanisms mediating the effects of CB2 receptor stimulation on hepatic fibrosis. They are probably related to the strong abundance of these receptors in nonparenchymal and biliary cells located within and at the edges of fibrotic septa that directly mediate growth arrest and antifibrotic and proapoptotic actions in hepatic cells (Julien et al., 2005; Liu et al., 2008). Whatever the case, however, our results indicate that selective pharmacological activation of the CB2 receptor is effective in preventing fibrosis progression in experimental liver disease.

There is much experimental evidence indicating that the hepatic apelin system is an important mediator of the initiation and maintenance of the inflammatory and fibrogenic processes occurring in the cirrhotic liver (Principe et al., 2008; Melgar-Lesmes et al., 2010, 2011). In fact, AP is selectively expressed in HSCs of humans and rats with cirrhosis and markedly stimulates PDGFRβ, collagen type 1 (Col1), and cell viability in LX-2 cells, a human cell line of activated stellate cells. In contrast, APJ blockade significantly regressed hepatic fibrosis and angiogenesis in cirrhotic animals and prevented the induction of PDGFRβ and Col1 expression induced by profibrogenic agents in LX-2 cells. In the current investigation, we chemically disrupted APJ signaling using F13A. This is an analog of apelin-13 in which the phenylalanine at the C terminus of the peptide is substituted by an alanine residue that behaves as an AP-specific antagonist (Melgar-Lesmes et al., 2010). Interaction of this competitive antagonist with APJ fully abolishes the biological activity of AP (Lee et al., 2005).

Acquisition of a proliferative, proinflammatory, and contractile phenotype by quiescent stellate cells is the most characteristic response of activated HSCs to chronic liver injury. Our experiments indicate that the APJ antagonist exerts its antifibrogenic effect by acting on different steps of this process. Chronic administration of F13A strongly reduced α-SMA, a well accepted marker of hepatic myofibroblasts, suggesting that APJ antagonism in vivo represses the activation of HSCs in CCl_4-treated rats.

The current investigation indicates that in addition to favoring cell viability, CB2 stimulation or APJ blockade also interferes with the production of profibrogenic mediators produced during chronic liver injury and the concomitant tissue repair. In this regard, the inhibitory effect on PDGF signaling shared by both AM1241 and F13A is noteworthy, considering that PDGF is the most potent proproliferative cytokine for HSCs (Pinzani et al., 1989; Friedman, 2008).

Pharmacological stimulation of the CB2 receptor or inhibition of AP activity also appears to affect the synthesis of molecules implicated in ECM remodeling. The net deposition of scar tissue depends on the balance between synthesis and degradation. The latter reflects the relative activity of MMPs and their inhibitor TIMPs, which are mainly produced by HSCs and other inflammatory cells (Iredale, 2007; Friedman, 2008). In experimental and human cirrhosis, fibrosis appears to be the result not only of excessive ECM synthesis but also of reduced degradation, which is caused by the up-regulation of TIMPs, inactivating the concurrently secreted MMPs (Iredale, 2007). According to these mechanisms, the untreated fibrotic rats in our experiments presented a marked induction of Col1α2 gene expression as well as a significant up-regulation of the MMPs. This result can be explained as a compensatory mechanism designed to eliminate the excess of scar tissue. However, the concomitant TIMP induction overwhelmed MMP activity, thereby leading to a net ECM deposition in the liver. ECM remodeling is indeed regulated by the balance between MMPs and TIMPs rather than by their absolute levels (Iredale, 2007). Therefore, several investigations have proposed that the inhibitory activity of TIMPs is the leading regulator of the remodeling process (Arthur,

2000; Iredale, 2007). In our study, treatment with both AM1241 and F13A was associated with a significant increase in the MMP/TIMP ratio in agreement with the inhibition of fibrosis progression. This altered balance was due to TIMP1 inhibition rather than to a further activation of MMPs and further supports the concept that TIMP activity is a major regulator of the ECM degradation pattern in the injured liver by controlling the activity of the secreted MMPs.

Tissue repair is a homeostatic response toward tissue injury, in which multiple and complex proinflammatory, proangiogenic, and profibrogenic processes are activated. In the liver, maintenance of tissue aggression results in the perpetuation of these phenomena, the wound-healing response progressively leading to advanced fibrosis and eventually cirrhosis. Breaking this vicious circle is a major challenge to stopping fibrosis in patients with liver disease. In the current investigation, we have shown that stimulation of CB2 receptors or blocking the activity of the hepatic apelin system is able to attenuate collagen deposition in CCl_4-treated rats through common mechanisms. In fact, despite the marked differences in the signaling pathways driving endocannabinoids and AP antifibrogenic effects, both inhibit PDGFRβ expression and alter MMP/TIMP balance by decreasing TIMP1 messenger and protein abundance. These results, therefore, point to PDGF signaling and TIMP1 activity as major targets for future antifibrotic therapies.

Authorship Contributions

Participated in research design: Reichenbach, Ros, Melgar-Lesmes, and Jiménez.

Conducted experiments: Reichenbach, Ros, Fernández-Varo, Casals, and Campos.

Contributed new reagents or analytic tools: Makriyannis.

Performed data analysis: Reichenbach, Ros, and Morales-Ruiz.

Wrote or contributed to the writing of the manuscript: Reichenbach, Fernández-Varo, Jiménez, Casals, and Morales-Ruiz.

References

Akhmetshina A, Dees C, Busch N, Beer J, Sarter K, Zwerina J, Zimmer A, Distler O, Schett G, and Distler JH (2009) The cannabinoid receptor CB2 exerts antifibrotic effects in experimental dermal fibrosis. *Arthritis Rheum* **60:**1129–1136.

Arthur MJ (2000) Fibrogenesis II. Metalloproteinases and their inhibitors in liver fibrosis. *Am J Physiol Gastrointest Liver Physiol* **279:**G245–G249.

Clària J and Jiménez W (1999) Renal dysfunction and ascites in carbon tetrachloride-induced cirrhosis in rats, in *The Liver and the Kidney* (Arroyo V, Schrier RW, Rodés J, and Ginès P eds) pp 379–396, Blackwell Science, Boston.

Daviaud D, Boucher J, Gesta S, Dray C, Guigne C, Quilliot D, Ayav A, Ziegler O, Carpene C, Saulnier-Blache JS, et al. (2006) TNF-α up-regulates apelin expression in human and mouse adipose tissue. *FASEB J* **20:**1528–1530.

Deveaux V, Cadoudal T, Ichigotani Y, Teixeira-Clerc F, Louvet A, Manin S, Nhieu JT, Belot MP, Zimmer A, Even P, et al. (2009) Cannabinoid CB2 receptor potentiates obesity-associated inflammation, insulin resistance and hepatic steatosis. *PLoS One* **4:**e5844.

Friedman SL (2008) Hepatic stellate cells: protean, multifunctional, and enigmatic cells of the liver. *Physiol Rev* **88:**125–172.

Friedman SL (2010) Evolving challenges in hepatic fibrosis. *Nat Rev Gastroenterol Hepatol* **7:**425–436.

Gressner OA, Weiskirchen R, and Gressner AM (2007) Evolving concepts of liver fibrogenesis provide new diagnostic and therapeutic options. *Comp Hepatol* **6:**7.

Hézode C, Zafrani ES, Roudot-Thoraval F, Costentin C, Hessami A, Bouvier-Alias M, Medkour F, Pawlostky JM, Lotersztajn S, and Mallat A (2008) Daily cannabis use: a novel risk factor of steatosis severity in patients with chronic hepatitis C. *Gastroenterology* **134:**432–439.

Horváth B, Magid L, Mukhopadhyay P, Bátkai S, Rajesh M, Park O, Tanchian G, Gao RY, Goodfellow CE, Glass M, et al. (2011) A new cannabinoid 2 receptor agonist HU-910 attenuates oxidative stress, inflammation, and cell death associated with hepatic ischemia/reperfusion injury. *Br J Pharmacol* doi:10.1111/j. 1476-5381.2011.01381.x.

Ibrahim MM, Deng H, Zvonok A, Cockayne DA, Kwan J, Mata HP, Vanderah TW, Lai J, Porreca F, Makriyannis A, et al. (2003) Activation of CB2 cannabinoid receptors by AM1241 inhibits experimental neuropathic pain: pain inhibition by receptors not present in the CNS. *Proc Natl Acad Sci USA* **100:**10529–10533.

Iredale JP (2007) Models of liver fibrosis: exploring the dynamic nature of inflammation and repair in a solid organ. *J Clin Invest* **117:**539–548.

Jeong WI, Osei-Hyiaman D, Park O, Liu J, Bátkai S, Mukhopadhyay P, Horiguchi N, Harvey-White J, Marsicano G, Lutz B, et al. (2008) Paracrine activation of hepatic CB1 receptors by stellate cell-derived endocannabinoids mediates alcoholic fatty liver. *Cell Metab* **7:**227–235.

Jimenez W, Parés A, Caballería J, Heredia D, Bruguera M, Torres M, Rojkind M, and Rodés J (1985) Measurement of fibrosis in needle liver biopsies: evaluation of a colorimetric method. *Hepatology* **5:**815–818.

Julien B, Grenard P, Teixeira-Clerc F, Van Nhieu JT, Li L, Karsak M, Zimmer A, Mallat A, and Lotersztajn S (2005) Antifibrogenic role of the cannabinoid receptor CB2 in the liver. *Gastroenterology* **128:**742–755.

Lee DK, Saldivia VR, Nguyen T, Cheng R, George SR, and O'Dowd BF (2005) Modification of the terminal residue of apelin-13 antagonizes its hypotensive action. *Endocrinology* **146:**231–236.

Liu HY, Yang Q, Duan RX, Zhang YW, and Tang WX (2008) [Effects of anandamide on the activation and proliferation of hepatic stellate cells through cannabinoid-2 receptors]. *Zhonghua Gan Zang Bing Za Zhi* **16:**430–434.

Malan TP Jr, Ibrahim MM, Deng H, Liu Q, Mata HP, Vanderah T, Porreca F, and Makriyannis A (2001) CB2 cannabinoid receptor-mediated peripheral antinociception. *Pain* **93:**239–245.

Marra F (1999) Hepatic stellate cells and the regulation of liver inflammation. *J Hepatol* **31:**1120–1130.

Masri B, Morin N, Cornu M, Knibiehler B, and Audigier Y (2004) Apelin (65–77) activates p70 S6 kinase and is mitogenic for umbilical endothelial cells. *FASEB J* **18:**1909–1911.

Melgar-Lesmes P, Casals G, Pauta M, Ros J, Reichenbach V, Bataller R, Morales-Ruiz M, and Jimenez W (2010) Apelin mediates the induction of profibrogenic genes in human hepatic stellate cells. *Endocrinology* **151:**5306–5314.

Melgar-Lesmes P, Pauta M, Reichenbach V, Casals G, Ros J, Bataller R, Morales-Ruiz M, and Jiménez W (2011) Hypoxia and proinflammatory factors upregulate apelin receptor expression in human stellate cells and hepatocytes. *Gut* **60:**1404–1411.

Morales-Ruiz M and Jiménez W (2005) Neovascularization, angiogenesis, and vascular remodelling in portal hypertension, in *Portal Hypertension: Pathobiology, Evaluation, and Treatment* (Sanyal AJ, Shah VH eds) pp 99–112, Humana Press, Totowa, NJ.

Muñoz-Luque J, Ros J, Fernández-Varo G, Tugues S, Morales-Ruiz M, Alvarez CE, Friedman SL, Arroyo V, and Jiménez W (2008) Regression of fibrosis after chronic stimulation of cannabinoid CB2 receptor in cirrhotic rats. *J Pharmacol Exp Ther* **324:**475–483.

Pacher P, Bátkai S, and Kunos G (2006) The endocannabinoid system as an emerging target of pharmacotherapy. *Pharmacol Rev* **58:**389–462.

Pinzani M, Gesualdo L, Sabbah GM, and Abboud HE (1989) Effects of platelet-derived growth factor and other polypeptide mitogens on DNA synthesis and growth of cultured rat liver fat-storing cells. *J Clin Invest* **84:**1786–1793.

Principe A, Melgar-Lesmes P, Fernández-Varo G, del Arbol LR, Ros J, Morales-Ruiz M, Bernardi M, Arroyo V, and Jiménez W (2008) The hepatic apelin system: a new therapeutic target for liver disease. *Hepatology* **48:**1193–1201.

Reichenbach V, Ros J, and Jiménez W (2010) Endogenous cannabinoids in liver disease: many darts for a single target. *Gastroenterol Hepatol* **33:**323–329.

Ros J, Fernández-Varo G, Muñoz-Luque J, Arroyo V, Rodés J, Gunnet JW, Demarest KT, and Jiménez W (2005) Sustained aquaretic effect of the V2-AVP receptor antagonist, RWJ-351647, in cirrhotic rats with ascites and water retention. *Br J Pharmacol* **146:**654–661.

Tam J, Liu J, Mukhopadhyay B, Cinar R, Godlewski G, and Kunos G (2011) Endocannabinoids in liver disease. *Hepatology* **53:**346–355.

Teixeira-Clerc F, Julien B, Grenard P, Tran Van Nhieu J, Deveaux V, Li L, Serriere-Lanneau V, Ledent C, Mallat A, and Lotersztajn S (2006) CB1 cannabinoid receptor antagonism: a new strategy for the treatment of liver fibrosis. *Nat Med* **12:**671–676.

Tugues S, Fernandez-Varo G, Muñoz-Luque J, Ros J, Arroyo V, Rodés J, Friedman SL, Carmeliet P, Jiménez W, and Morales-Ruiz M (2007) Antiangiogenic treatment with sunitinib ameliorates inflammatory infiltrate, fibrosis, and portal pressure in cirrhotic rats. *Hepatology* **46:**1919–1926.

Yao BB, Mukherjee S, Fan Y, Garrison TR, Daza AV, Grayson GK, Hooker BA, Dart MJ, Sullivan JP, and Meyer MD (2006) *In vitro* pharmacological characterization of AM1241: a protean agonist at the cannabinoid CB2 receptor? *Br J Pharmacol* **149:**145–154.

Address correspondence to: Dr. Wladimiro Jiménez, Servicio de Bioquímica y Genética Molecular, Hospital Clínic Universitari, Villarroel 170, Barcelona 08036, Spain. E-mail: wjimenez@clinic.ub.es